

Azolla Pinnata: Sustainable Floating Oil Cleaner of Water Bodies

Ghulam Mohd, Irfan Majeed Bhat, Insha Kakroo, Akshay Balachandran, Ruheena Tabasum, Kowsar Majid, Mohammad Farooq Wani, Uttam Manna, Gajanan Ghodake, and Saifullah Lone*

Cite This: *ACS Omega* 2024, 9, 12725–12733

Read Online

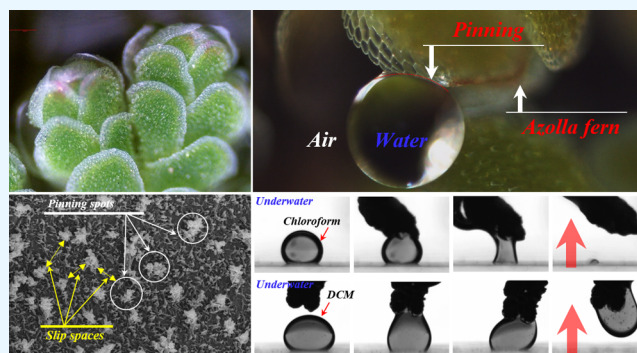
ACCESS |

Metrics & More

Article Recommendations

Supporting Information

ABSTRACT: Various plant-based materials effectively absorb oil contaminants at the water/air interface. These materials showcase unparalleled efficiency in purging oil contaminants, encompassing rivers, lakes, and boundless oceans, positioning them as integral components of environmental restoration endeavors. In addition, they are biodegradable, readily available, and eco-friendly, thus making them a preferable choice over traditional oil cleaning materials. This study explores the phenomenal properties of the floating Azolla fern (*Azolla pinnata*), focusing on its unique hierarchical leaf surface design at both the microscale and nanoscale levels. These intricate structures endow the fern with exceptional characteristics, including superhydrophobicity, high water adhesion, and remarkable oil or organic solvent absorption capabilities. Azolla's leaf surface exhibits a rare combination of dual wettability, where hydrophilic spots on a superhydrophobic base enable the pinning of water droplets, even when positioned upside-down. This extraordinary property, known as the parahydrophobic state, is rare in floating plants, akin to the renowned *Salvinia molesta*, setting Azolla apart as a natural wonder. Submerged in water, Azolla leaves excel at absorbing light oils at the air–water interface, demonstrating a notable ability to extract high-density organic solvents. Moreover, Azolla's rapid growth, doubling in the area every 4–5 days, especially in flowing waters, positions it as a sustainable alternative to traditional synthetic oil-cleaning materials with long-term environmental repercussions. This scientific lead could pave the way for more environmentally friendly approaches to mitigate the negative impacts of oil spills and promote a cleaner water ecosystem.



1. INTRODUCTION

The relationship between water and climate change is complex and multifaceted. The discharge of oils and organic solvents into water bodies is a serious environmental issue of widespread concern, causing harm to marine ecosystems and threatening the livelihoods of coastal communities.¹ Besides, oils also destroy the protective capability of fur-bearing creatures, including otters and bird feathers with hydrophobic surface features,^{1,2} thus exposing the valuable creations to tough rudiments.³ On losing water-repellent character on skin and feathers, the birds/and animals die from hypothermia.⁴ Besides, the investigation into the earlier oil leaks revealed that some deadly toxic substances have stayed in marine waters for centuries (International Energy Agency).⁵ Some long-term effects may include population declines, reduced biodiversity, and altered community structures.^{6,7}

Materials and techniques for oil spill cleanup vary based on factors like spill size, location, oil type, and weather.^{8–10} The use of nonbiodegradable oil cleaners, such as pads, socks, and booms made of foam, rubber, or plastic, in oil spill cleanup has inherent drawbacks. Additionally, in situ burning, though rapid in removing large oil volumes, emits harmful substances, and vacuum trucks, while efficient in extraction, produce harmful

emissions during the process. These limitations underscore the need for exploring more environmentally friendly alternatives to mitigate the adverse impact of oil spill cleanup on ecosystems. Plant-based materials like coconut coir/or biochar efficiently absorb oil and clean up oil spills.^{11,12} These materials have high absorption rates and can effectively remove oil from the water and soil. In addition, they are biodegradable and eco-friendly, making them a more sustainable alternative to traditional oil cleaning methods.^{13,14}

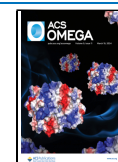
Water and oil are separated at the interface between the water and solid surfaces. The interaction of water molecules with nano-/or microscale surface topography and functionality is crucial in oil/water separation.^{15–17} The chemical and physical properties governing the interaction between water and the solid are surface energy, hydrophobicity/or hydrophilicity, and surface charge.^{18–20} This interaction can impact

Received: October 25, 2023

Revised: February 5, 2024

Accepted: February 12, 2024

Published: March 7, 2024



the behavior of substances dissolved or suspended in water.²¹ Particularly, understanding the water/solid interface is vital for oil/water filters/membranes.^{22,23}

This study presents a comprehensive analysis of the Azolla fern (*Azolla pinnata*) found in lake waters, highlighting its exceptional oil-absorbing properties. A thorough examination of the surface structural intricacies of the fern leaves has unveiled a remarkable hierarchical design featuring microscale and nanoscale structures. These structures impart dual functionality, effectively repelling water while attracting oil—a phenomenon of great scientific interest. The study employed microscopic techniques, real-time optical visualization, contact angle (C.A.) analysis, and water droplet adhesive force measurements to investigate the correlation between the surface structure of the fern and its ability to absorb oil from water. The findings could offer a scientific lead in confronting oil spill issues by floating plant species for sustainable oil remediation. The fern grows very fast and provides an opportunity to be cultivated and deployed in areas affected by oil spills to accelerate the natural biodegradation process. In addition to their potential remediation capabilities, living floating species offer other benefits. They can help restore damaged ecosystems by providing a food source for higher trophic levels, and they may also have applications in bioremediation beyond oil spills such as in treating wastewater or other pollutants.

2. EXPERIMENTAL WORK

2.1. Materials and Sample Collection. Various oils and organic solvents were used during the experiments: crude oil (Hindustan petroleum), mustard oil (p-mark, grade-1), soybean oil (fortune, grade-1), toluene (RANKEM), diesel (RANKEM), chloroform (CDH), and dichloromethane (RANKEM). The Azolla fern samples were collected from Dal Lake, Srinagar, India. The fresh samples were washed with tap water before use. The samples remained fresh in a Petri dish filled with tap water at laboratory temperature for several months. We investigated only the upper floating part of the fern; we were not interested in the submerged roots.^{24–26} The Azolla plant is readily available in Dal Lake in Srinagar; it overgrows in the areas of slow-moving waters in late summer before withering in the freezing winter temperatures. Three kinds of oils and four different organic solvents of varying viscosity (η) and density (ρ) were used. For instance, crude oil, $\eta = 222.29$ mPa s and $\rho = 0.8$ g/mL at 15 °C; mustard oil, $\eta = 11.727$ mPa s and $\rho = 0.96$ g/mL at 20 °C; soybean oil, $\eta = 60.9$ mPa s and $\rho = 0.91$ g/mL at 20 °C; toluene, $\eta = 0.63$ mPa s and $\rho = 0.86$ g/mL at 20 °C; diesel, $\eta = 3.16$ mPa s and $\rho = 0.88–0.82$ g/mL at 15 °C; chloroform, $\eta = 0.536$ mPa s and $\rho = 1.48$ g/mL at 20 °C; and dichloromethane, $\eta = 0.41$ mPa s and $\rho = 1.33$ g/mL at 25 °C.

3. EXPERIMENTAL WORK

3.1. Azolla Fern Habitat and Dimensions. *A. pinnata* (known as the mosquito fern, feathered mosquito fern, duckweed fern, and water velvet) is a floating fern.²⁷ It is a species of the Salviniaceae family native to Asia (India, China, Korea, Japan, Brunei Darussalam, and the Philippines), Africa, and parts of Australia. The aquatic plant grows on the water's surface, covering the entire area with a green and reddish carpet-like appearance. The plant thrives on quiet, slow-moving bodies of water. It is found to double its biomass in 1.9

days, with most strains achieving such growth within a week under optimal conditions.²⁷ The fern has a triangular stem (2.5 cm long) with various overlapping angular leaves (1/or 2 cm long). The leaves are initially green, turning blue-green and dark red within a few months.²⁸ The floating character of the fern is blamed on the tiny structures on the leaf that repel water; however, this water-repelling character is not discussed adequately.²⁹ Moreover, symbionts (cyanobacterium *Anabaena azollae*) on leaves fix atmospheric nitrogen. Therefore, the plant can grow in habitats that are nitrogen-deficient.³⁰ The plant can also adsorb heavy metals (e.g., lead) from wastewater.

A digital camera and an optical microscope (LEICA, DM-600M, Germany) were used to study the general morphology and the water droplet interaction with the Azolla fern surface (Figure 1). We observed that the small/or large water droplets interact differently with the fern surface.

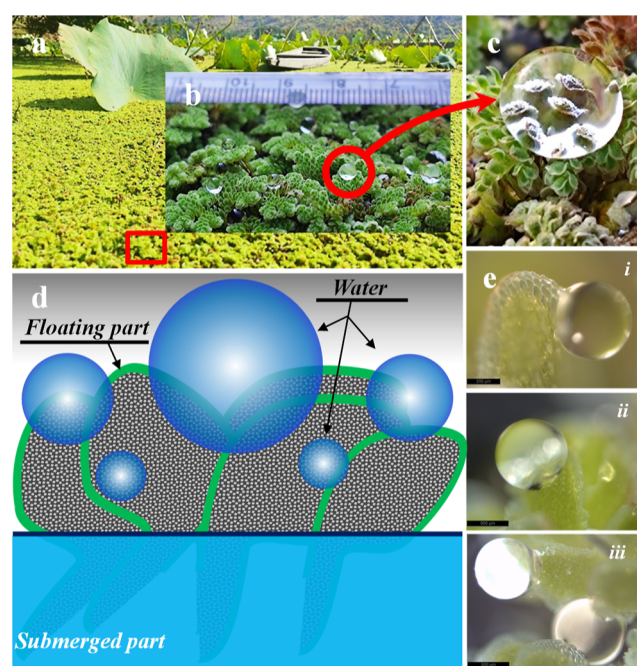


Figure 1. *A. pinnata* fern habitat and parahydrophobic features. (a) Floating Azolla fern in Dal Lake of Srinagar. Inset: high magnification of the plant. (b) Digital image of a gigantic spherical water droplet on the fern leaves showing water repellency. (c) High-resolution digital photograph of the water droplet. (d) Schematic of the Azolla fern showing two critical parts of the plant (i.e., floating and submerged). (e) Optical microscopic images of the spherical water droplets pinning to the surface of the fern leaves at different angles (i, ii, and iii) to demonstrate the parahydrophobic surface topography features.

3.2. Tunable Water Adhesion on the Azolla Fern. The wetting phenomenon of water on the Azolla fern surface is tested by C.A. analysis. Employing an electronic syringe connected to a C.A. goniometer, we strategically positioned D.I. water droplets on various surface locations. The static contact angle (SCA) measured is found at 152° (ACAM-Series, Apex Instruments, India), Figure 3d. Depending on the volume, the water drops pin or slip off the surface at various sliding angles. For a more comprehensive visual representation of these wetting behaviors and to access the associated data, see Table 1.

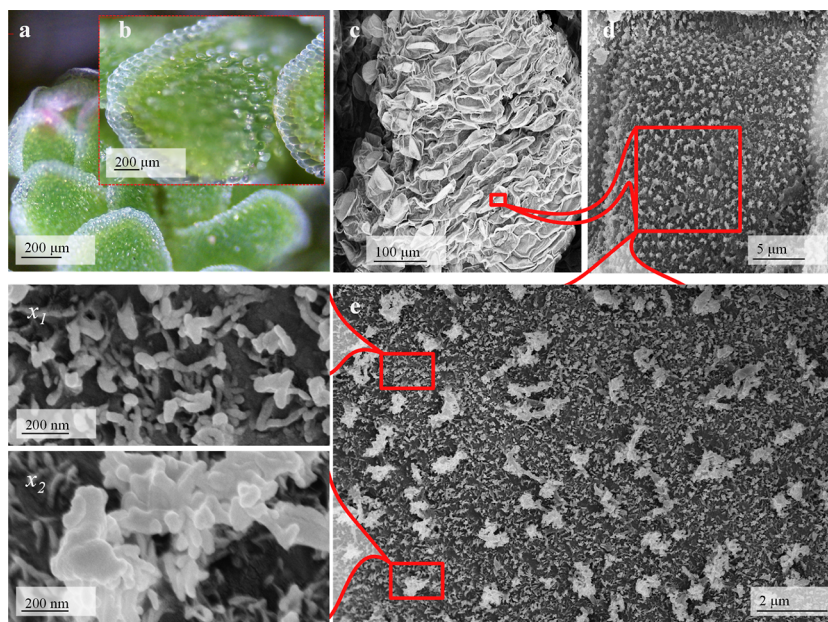


Figure 2. Hierarchical surface structure of *A. pinnata*. (a) Optical micrographs of the plant leaves; inset: high-magnification optical image of the leaf surface (b). (c) SEM images of the leaf surface displaying multiple airlike sacs. (d) SEM image illustrating each air sac adorned with a carpet of microscale and nanoscale structures. (e) High-resolution SEM image depicting the hierarchical structures (x_1 : hydrophobic structure, x_2 : hydrophilic structure).

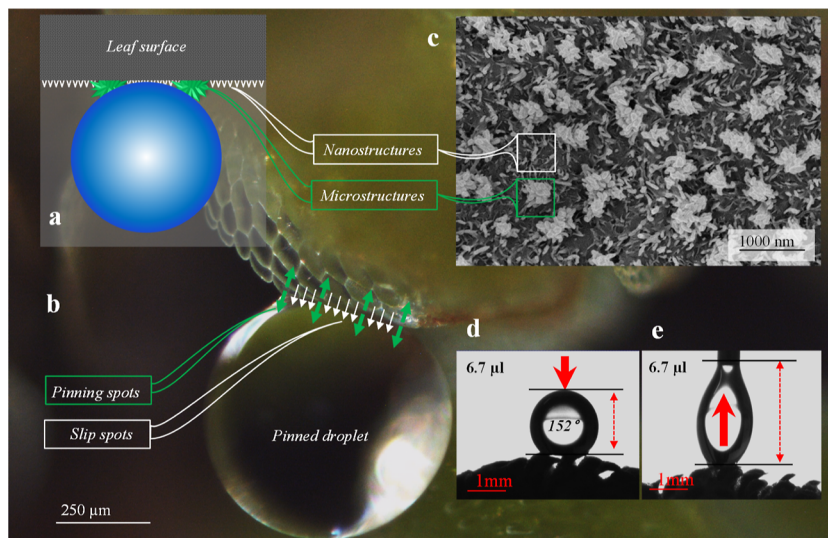


Figure 3. Parahydrophobic Azolla fern leaf surface. (a) Representation of a water drop showing superhydrophobicity and high-adhesion behavior on the fern leaf (the Cassie-impregnating wetting state). (b) Optical microscopic image of a water drop pinned to a leaf upside-down. (c) SEM image showing rough microstructures and smooth nanobases on the surface for water pinning and repelling features. (d) Optical images of a water drop showing a high SCA of 152° and the (e) pinning effect of the water drop on detaching it from the leaf surface.

Table 1. Sliding Angle Impact on the Pinning/Depinning of Water Drops of Variable Volumes

S/No	droplet volume (μL)	sliding angle (deg)	effect	sliding angle (deg)	effect
1	10 μL	$<5^\circ$	pinning	180°	pinning
2	20 μL	$<5^\circ$	pinning	180°	pinning
3	30 μL	$90\text{--}95^\circ$	pinning	$95\text{--}100^\circ$	slip
4	40 μL	$80\text{--}85^\circ$	pinning	$85\text{--}90^\circ$	slip
5	50 μL	$<5^\circ$	slip	$5\text{--}10^\circ$	slip

3.3. Tunable Water Adhesion on the Azolla Fern. The adhesive force between water droplets and the surface of Azolla

leaves is investigated by using a force tensiometer (KRUSS, Force Tensiometer-K100, Germany). This analytical instrument allows for the precise measurement and analysis of interfacial forces. Notably, it has been observed that the volume of the water droplets notably influences the adhesive forces. A systematic experimental approach is employed in studying the efficacy of Azolla leaves in removing oil from water. Initially, Azolla leaves are affixed to a linear stage, which allows for controlled movement. The Azolla leaves are progressively introduced into oil-contaminated water, facilitating contact with the oil droplets. Subsequently, the leaves are carefully withdrawn. The process is meticulously monitored

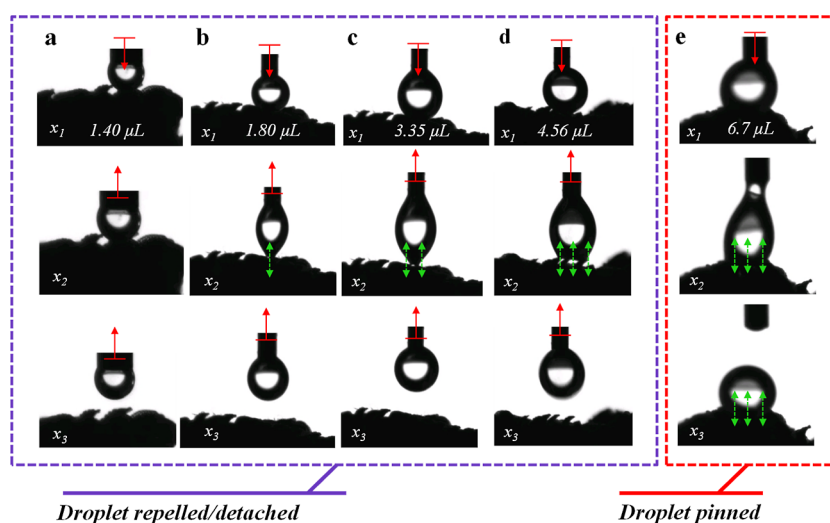


Figure 4. Optically monitoring the place-and-pick experiment. (a–d) Water droplets (with volumes ranging between 1.4 and 4.5 μL) are placed and picked from the surface. (e) Water drops (with a volume of 6.7 μL) remain pinned to the surface.

and recorded using a high-speed camera, specifically an ACAM-Series camera provided by Apex Instruments in India. This scientific methodology provides insight into the adhesive properties of Azolla leaves. It offers a systematic means of investigating their potential application in oil removal from water, which holds significance in environmental and ecological contexts (Figure 3).

3.4. Scanning Electron Microscopy. The morphological characteristics of the Azolla fern leaf surface, particularly at the micro- and nanoscale levels, are examined using field emission scanning electron microscopy (FESEM) with a ZEISS GeminiSEM-500 instrument in Germany. While effective in capturing the overall structure, traditional optical microscopy (OM) and digital imaging techniques were limited in revealing the intricate topographical features on the leaf's surface. Both OM and digital imagery depicted the Azolla leaves as having a gently curved shape with microsized protrusions distributed across the leaf surface. However, the finer microscale/nanoscale topographical details, crucial for understanding surface properties at the nanoscale level, were beyond the resolution capabilities of these conventional techniques. In contrast, the utilization of FESEM brought to light these minuscule surface intricacies, as illustrated in Figure 4. FESEM's exceptional resolution and imaging capabilities uncovered the previously unseen micro- and nanoscale topographical features present on the Azolla fern leaf, offering a comprehensive insight into its surface structure. This in-depth examination is vital in understanding the leaf's functional attributes and potential applications in various scientific and environmental contexts.

4. RESULTS AND DISCUSSION

4.1. Hierarchical Structural Details. In preparation for the FESEM analysis, the surfaces under investigation underwent a crucial pretreatment process. Initially, a nanolayer of gold with nanosized particles, approximately 10–9 nm in diameter, was meticulously deposited onto the surface. This deposition occurred under controlled conditions, specifically at a temperature of 20 $^{\circ}\text{C}$ and a pressure of 10–6 mbar. Upon closer examination using FESEM, the coated surface revealed a fascinating and intricate hierarchical structure.

The surface structure is divided into two distinctive components: (a) smooth nanostructures (surface base): a uniform array of nanostructures characterizes the foundation of the Azolla leaf surface. However, these structures played a crucial role in determining the surface's hydrophobic properties at the nanoscale. Their uniformity and arrangement connect to what is referred to as the "depinning effect", indicating that they actively prevent the pinning of water droplets on the surface. This hydrophobic behavior stems from the regular, smooth nature of these nanostructures. (b) Irregular microstructures: Complementing the smooth nanostructures were randomly spaced, irregular microstructures on the surface. These larger-scale structures exhibited a contrasting hydrophilic nature. In other words, they had an affinity for water and actively participated in the pinning of water droplets. These irregular microstructures created hydrophilic domains on the surface, which allowed water droplets to adhere to them. As depicted in Figure 2, the interplay between the hydrophobic smooth nanostructures and the hydrophilic irregular microstructures is central to the surface's wetting behavior. This complex, dual-scale surface architecture contributes to the material's overall wetting characteristics and has implications for its potential applications in various scientific and technological contexts.

4.2. Water Drop Pinning and Depinning Effects. The multiscale surface structures of the Azolla leaf show highly adhesive superhydrophobic features (i.e., the rose petal effect). The two effects are schematically illustrated and optically confirmed (Figure 3a,b). While checking the SEM image, one could correlate the two effects to microstructures and nanostructures (Figure 3c). On testing the water-wetting properties on the Azolla leaf surface, we found that the SCA of the water drop on the leaf surface is $>152^{\circ}$ (Figure 3d). Besides maintaining the spherical shape on the leaf surface, the water drop remains pinned to the surface (even in an upside-down position) by high adhesive forces. The increased C.A. is due to the smooth nanostructures. The pinning effect is blamed on sharp, irregular microstructures that pierce into the water droplet. The water drop exhibited a stretching effect on detaching from the leaf surface to confirm the pinning phenomenon, Figure 3e. Such surfaces (with superhydrophobic features and high adhesive forces) are called para-

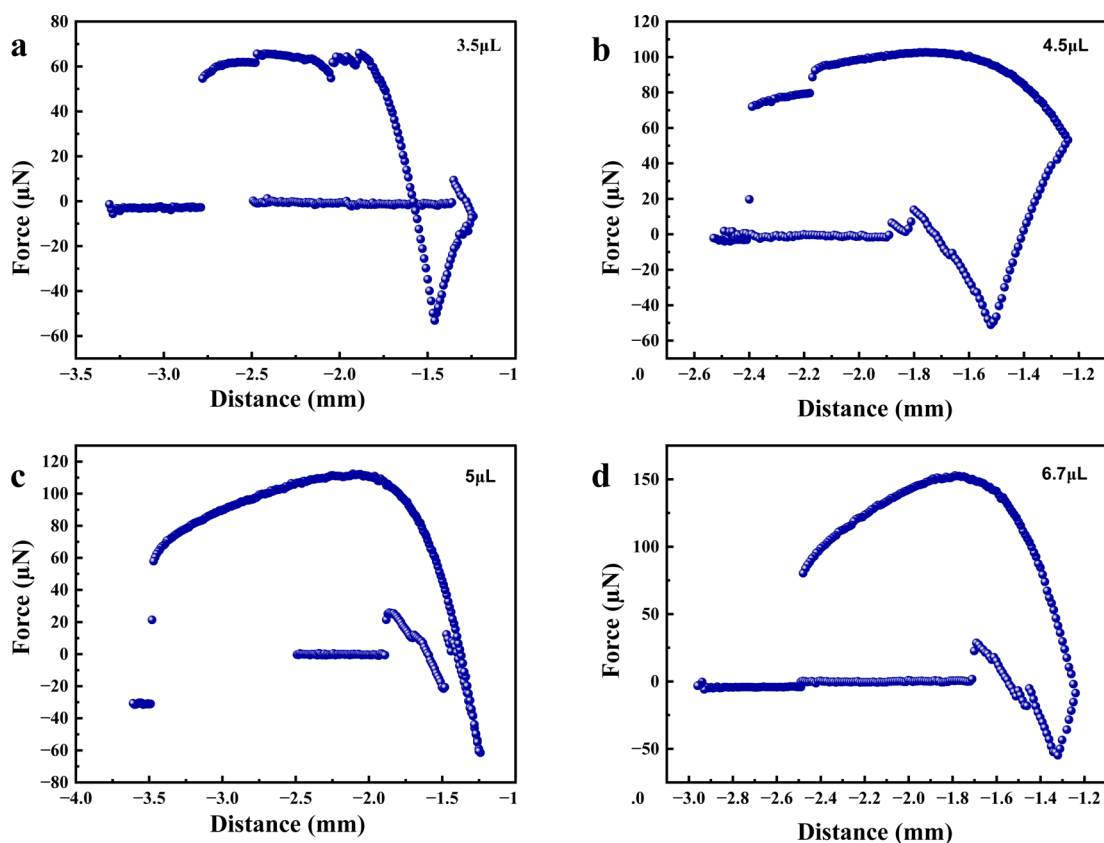


Figure 5. Force–distance curves. Adhesive force measurement of water drops on the adaxial surface of the Azolla fern as a function of the droplet volume (a–d; between 3.5 and 6.7 μL).

hydrophobic surfaces. A few common examples of such surfaces are rose petals and *Salvinia molesta*.³¹ The parahydrophobic surfaces are explored for application in separation, directional transport of liquids, water collection, bubble nucleation, or departure during boiling. Generally, the theoretical explanation of surfaces with an SCA greater than 150° is termed superhydrophobic surfaces. Nevertheless, superhydrophobic surfaces could be explained in two ways: (a) liquid touching the solid surface (i.e., Wenzel's state) to explain homogeneous wetting,³² which is described by eq 1

$$\cos \theta_{\text{wca}} = r \cos \theta_{\text{yca}} \quad (1)$$

where θ_{wca} is the Wenzel C.A., θ_{yca} is the Young C.A., and r is the roughness ratio (i.e., the ratio of the actual area to the calculated area of the solid surface wetted by liquid). (b) Air film traps between liquid and solid surfaces (Cassie's state), which represents heterogeneous wetting,³³ as explained by eq 2

$$\cos \theta_{\text{cca}} = rf \cos \theta_{\text{yca}} + f - 1 \quad (2)$$

where θ_{cca} is the Cassie C.A., θ_{yca} is the Young C.A., r is the ratio of the actual area to the calculated area of the solid surface wetted by liquid, and f denotes the area fraction of the estimated wet area. This condition matches the lotus effect; the three contact lines are discontinuous, meaning the water droplets only make contact with the surface at a few discrete points rather than spread uniformly across the surface. This characteristic helps minimize the contact area between the water droplet and the surface, reducing adhesion and restricting water droplets from intruding into the microstructures. The situation promotes low C.A. hysteresis, and the

water droplets tend to bead up and roll freely in any direction. The low C.A. hysteresis means a minimum difference between the advancing C.A. (when the droplet is spreading) and the receding C.A. (when the droplet is retracting).

Overall, the combination of hydrophobicity, roughness, discontinuous contact lines, and low C.A. hysteresis allows water droplets to move freely on the surface, preventing the accumulation of dirt and ensuring self-cleaning properties (for instance, those observed on lotus leaves).^{34,35} Both Cassie and Wenzel states were thoroughly investigated previously. However, the parahydrophobic surface (a metastable state) can be described as an intermediate wetting state between the Cassie and Wenzel regimes. In this scenario, the three-phase contact line remains continuous, which refers to the water droplet spreading across the surface, making contact at multiple points instead of being localized at specific discrete points, as in the case of the Cassie state. The microstructures on the surface, which may bear ridges, pillars, or textures, generate strong capillary forces that pin the water droplet in place even when the surface is tilted, sliding, or inverted. Therefore, the surface demonstrates superhydrophobicity with high adhesive forces.^{36,37} The investigation of the parahydrophobic state is essential because it provides insights into the wetting phenomenon and the manipulation of liquid–solid interactions.³⁸

4.3. Water Drop Pinning and Depinning Effects. To illustrate the water pinning effect, which signifies the adhesive forces between water droplets and the Azolla leaf surface, we initially employed OM observation during a water drop placement and retrieval experiment. When tiny water droplets (ranging from 1.4 to 4.5 μL in volume) were placed on the

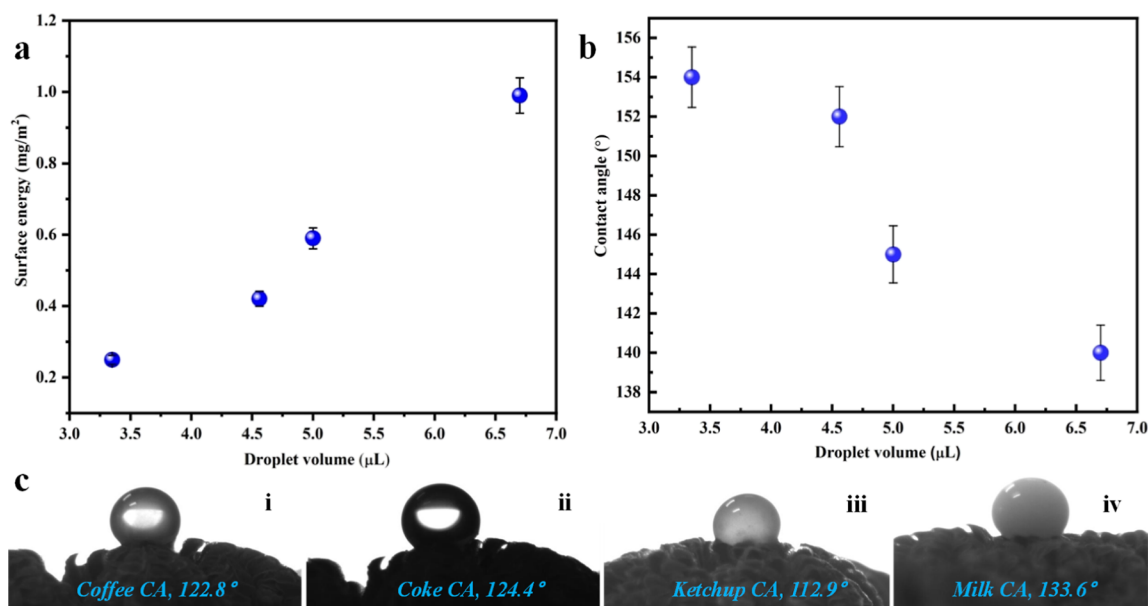


Figure 6. Plot of surface energy and SCA versus droplet volume. (a) Surface energy versus water drop volume. (b) SCA versus droplet volume. (c) SCA of various liquids.

surface, they could be effortlessly picked up vertically using a needle attached to an automated stage (as shown in Figure 4a–d). However, as the droplet volume increased to 6.7 μL , it exhibited a pronounced pinning effect, remaining firmly attached to the surface (as depicted in Figure 4e). This phenomenon underscores the intriguing water-adhesive properties of the Azolla leaf surface.

Second, we employed a force tensiometer to quantify the adhesive forces between the water droplet and the fern surface. This enabled us to probe these adhesive forces across a range of water droplet volumes. We observed a fascinating correlation: as the volume of the water droplets increased, the corresponding adhesive forces exhibited concurrent and substantial augmentation. This intriguing phenomenon is further elucidated through the representation of force–distance curves, graphically outlining the intricate interactions as the water droplet progressively approached and receded from the Azolla leaf surface, as showcased in the visual depiction found in Figure 5. These curves were recorded by using a force tensiometer, granting us invaluable insight into the dynamic interplay between the water droplets and the surface of the Azolla leaf.

During these interactions, the water droplets underwent continuous deformation as they approached the leaf's surface. However, the most intriguing aspect of this phenomenon was the gradual detachment of the droplets from the Azolla leaf. This detachment formed a distinct neck region—a slender, connecting bridge between the water droplets and the Azolla leaf. Notably, we observed multiple instances of these interactions across the surface of the Azolla leaf, each unveiling the complex interplay between the leaf surface and water droplets of varying volumes.

Our findings in this regard are especially noteworthy. When we examined water droplets measuring 6.7 μL in volume, we observed a substantial adhesive force quantified at 150 μN . This indicates a robust adhesive interaction between the water droplet and the Azolla leaf surface. In contrast, with water droplets of 3.5 μL in volume, the adhesive force measured 50

μN , representing a proportionally lower but still significant adhesive effect.

It means that the tiny water droplet on the Azolla leaf exhibits a much lower adhesive force on the surface than that of its bigger counterparts, as shown in Figure 4. When the water droplet volume is fixed at 3.35 μL , the SCA on the Azolla leaf is greater than $155^\circ \pm 1$. So, in this case, the water droplet cannot stick to the leaf surface, given that the water droplet is smaller in size and offers fewer pinning spots (i.e., irregular microstructures) to the water droplet. However, as the water droplet volume reaches 6.7 μL , the size of the droplet increases, and the SCA decreases to $140^\circ \pm 1$. Consequently, the droplet is pinned by surface microstructures (with a higher surface energy) at various spots, ensuring the stable attachment of the water droplet with the leaf surface (Figure 6a,b). Also, we investigated both the pinning and depinning of water droplets (with different volumes) on the leaf surface with different sliding angles on water droplets (with variable volumes) to illustrate the pinning effect.

We measured the SCA of various liquids on the fern leaf surface (Figure 6c). As the volume of droplets undergoes augmentation, three pivotal processes come into play, each playing a crucial role in the escalation of surface energy. First, the expansion in droplet size weakens the cohesive forces between its constituent molecules, thereby diminishing intermolecular interactions. This phenomenon leads to an expansion of the liquid–air interface, where these weakened intermolecular forces become influential. The consequence is a greater requirement for energy to maintain this enlarged surface area. Second, as the Laplace equation dictates, the pressure within a droplet exhibits an inverse relationship with its radius. With the growth of droplets, their internal pressure decreases, demanding higher pressures to maintain their characteristic spherical shape. An increase in surface energy accompanies this elevation in pressure. Lastly, from a thermodynamic perspective, it is inherently more energetically favorable for a liquid to occupy a smaller surface area owing to the reduced energy associated with cohesive forces. Hence, enlarging the volume of a droplet to more substantial

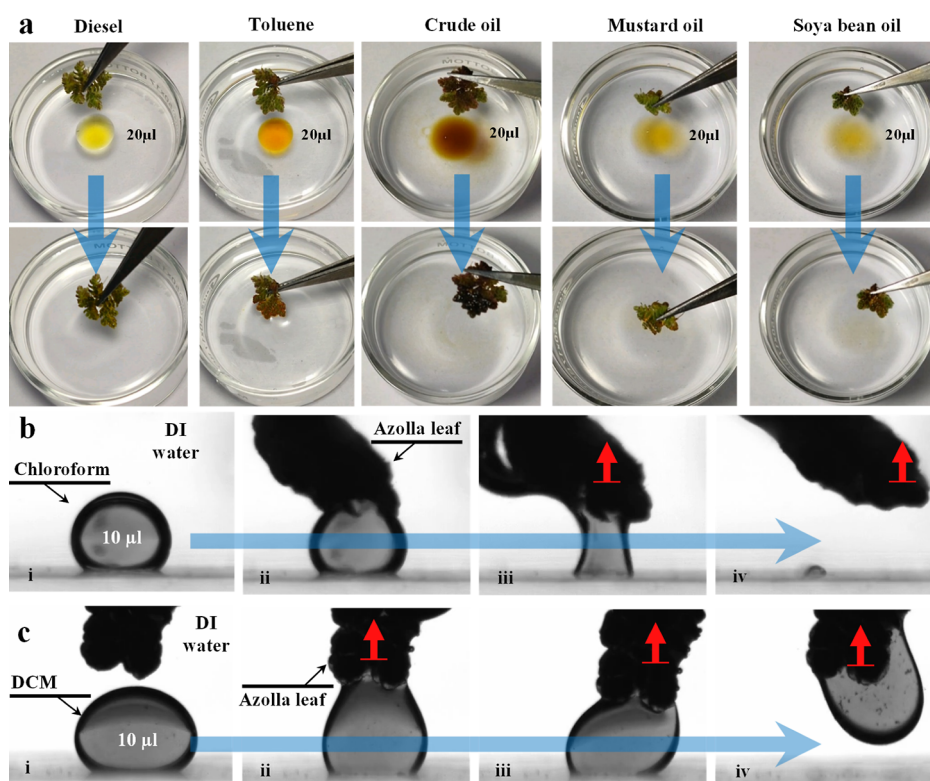


Figure 7. Remediation of oils and organic solvents by the Azolla leaf. (a) Removal of various oils (such as diesel, toluene, crude oil, mustard oil, and soybean oil) at the air/water interface and (b,c) organic solvents (dichloromethane (DCM) and chloroform) in an underwater condition.

proportions necessitates an increase in surface energy to sustain the expanded surface area. In summary, these three intricately interlinked processes collectively contribute to the overall augmentation of surface energy as the volume of the droplet experiences enlargement.

Further, we systematically examined the influence of the sliding angle on the pinning and depinning phenomena exhibited by water droplets, characterized by varying volumes, on the surface of Azolla fern leaves. The intricate hierarchical microscale and nanoscale structures inherent to the Azolla fern surface contribute to the manifestation of both pinning (manifesting adherence) and depinning (exhibiting superhydrophobicity). The pinning efficacy shows a notable dependence on the volume of the water droplets. Notably, as the droplet volume increases, the pinning action or the adhesive interaction undergoes a discernible weakening. For instance, water droplets with volumes ranging from 10 to 20 μL exhibit robust pinning, demonstrating the ability to adhere firmly even when positioned upside down (i.e., at 180°). However, as the droplet volume escalates to 30–40 μL , the pinning effect remains intact until the sliding angle reaches a transition zone between $90\text{--}95^\circ$ and $80\text{--}85^\circ$.

Moreover, an important observation arises when the water drop volume is further increased to 50 μL . At this threshold, the pinning effect on the leaf surface diminishes entirely, marking the onset of droplet slippage, which commences at a slight incline of less than 5° . Remarkably, with water droplets attaining volumes of 50 μL and beyond, the Azolla fern surface transitions to behaving akin to a lotus leaf, characterized by enhanced superhydrophobic properties. This transformation underscores the dynamic interplay between droplet volume and the structural attributes of the leaf surface, unraveling a nuanced understanding of the intricate wetting behaviors

exhibited by the Azolla fern (the summary of the investigation is given in Table 1).

4.4. Azolla Leaf Oil Separation on the Surface and Underwater. The mosquito ferns (*Azolla*) have a contrasting affinity toward water and oils, which means they are both superhydrophobic and superoleophilic in surface and underwater scenarios. Due to their hierarchical (i.e., micro-/nanoscale) surface structure, they repel water but quickly (i.e., in a couple of seconds) attract oils and organic solvents. Notably, they also clean up light oil drops from the surface of the water (Figure 7a), refer to Video S1 (Supporting Information), and suck heavy organic solvents from underwater conditions (Figure 7b). Also, refer to Video S2 (Supporting Information). The maximal absorption is attained in <12 s (for light oils), 25 s (for heavy oils), and <5 s (for organic solvents). These fundamental studies provide the first evidence of the enormous potential of floating fern leaves as selective oils/organic solvents absorbent in freshwater bodies. To investigate the impact of the physical oil qualities on the sorption capacity, we first assessed the sorption capacity of Azolla pinnate leaves with three different oils and four different organic solvents. For instance, crude oil, mustard oil, soybean oil, toluene, diesel, chloroform, and dichloromethane were used to make these measurements.

5. CONCLUSIONS

In summary, this study delves into the structural details of the Azolla fern, particularly its hierarchical design of leaves at the microscale and nanoscale levels. These unique structures give the fern distinct properties such as superhydrophobic surfaces, high water adhesion, and effective absorption of oils and organic solvents. The fern possesses a combination of hydrophilic spots (i.e., irregular microstructures) on a

superhydrophobic base (i.e., regular nanostructures), which results in high water adhesion on the superhydrophobic surface. Consequently, when a water droplet comes in contact with the fern's surface, the superhydrophobic base (with SCA > 150) shapes the droplet into a spherical form due to its low surface energy. In comparison, the hydrophilic spots pin the water droplet (even in an upside-down position) because of their high surface energy. This phenomenon is known as the rose-petal effect. The Azolla fern could act as a natural biodegradable material for oil remediation in various natural water bodies, such as rivers, lakes, and springs. It can absorb oil and organic solvents at the air/water surface and underwater. One of the notable advantages of using the Azolla fern as an oil cleaner is its availability, economical and environmentally friendly character, and quick growth in moving waters. The fern overgrows in a large chunk of water bodies, thus providing an alternative yet sustainable choice to traditional oil cleaning materials, often imposing long-term environmental impacts. Overall, the findings of this research have the potential to contribute to addressing oil spills by using floating plant species for sustainable oil remediation. Furthermore, since the fern is a millimeter in size and floats on an air/water surface, collecting ferns after cleaning is even easier. Hence, with our field experience and experimental results, we strongly recommend that the Azolla fern be grown with purpose within freshwater bodies to clean oils/or organic solvents.

■ ASSOCIATED CONTENT

SI Supporting Information

The Supporting Information is available free of charge at <https://pubs.acs.org/doi/10.1021/acsomega.3c08417>.

Oil and organic solvent absorption (MP4)

High-density organic solvent absorption in underwater conditions (MP4)

■ AUTHOR INFORMATION

Corresponding Author

Saifullah Lone – Department of Chemistry, National Institute of Technology (NIT), Jammu & Kashmir 190006 Srinagar, India; iDREAM (Interdisciplinary Division for Renewable Energy & Advanced Materials, Laboratory for Bioinspired Research on Advanced Interface and Nanomaterials (BRAINS), NIT, Jammu & Kashmir 190006 Srinagar, India; orcid.org/0000-0003-1026-7748; Email: saifullah.lone@nitsri.ac.in

Authors

Ghulam Mohd – Department of Chemistry, National Institute of Technology (NIT), Jammu & Kashmir 190006 Srinagar, India; iDREAM (Interdisciplinary Division for Renewable Energy & Advanced Materials, Laboratory for Bioinspired Research on Advanced Interface and Nanomaterials (BRAINS), NIT, Jammu & Kashmir 190006 Srinagar, India

Irfan Majeed Bhat – Department of Chemistry, National Institute of Technology (NIT), Jammu & Kashmir 190006 Srinagar, India; iDREAM (Interdisciplinary Division for Renewable Energy & Advanced Materials, Laboratory for Bioinspired Research on Advanced Interface and Nanomaterials (BRAINS), NIT, Jammu & Kashmir 190006 Srinagar, India

Insha Kakroo – Department of Chemistry, National Institute of Technology (NIT), Jammu & Kashmir 190006 Srinagar, India; iDREAM (Interdisciplinary Division for Renewable Energy & Advanced Materials, Laboratory for Bioinspired Research on Advanced Interface and Nanomaterials (BRAINS), NIT, Jammu & Kashmir 190006 Srinagar, India

Akshay Balachandran – Department of Chemistry, National Institute of Technology (NIT), Jammu & Kashmir 190006 Srinagar, India; iDREAM (Interdisciplinary Division for Renewable Energy & Advanced Materials, Laboratory for Bioinspired Research on Advanced Interface and Nanomaterials (BRAINS), NIT, Jammu & Kashmir 190006 Srinagar, India; orcid.org/0000-0002-6750-3206

Ruheena Tabasum – Department of Chemistry, National Institute of Technology (NIT), Jammu & Kashmir 190006 Srinagar, India; iDREAM (Interdisciplinary Division for Renewable Energy & Advanced Materials, Laboratory for Bioinspired Research on Advanced Interface and Nanomaterials (BRAINS), NIT, Jammu & Kashmir 190006 Srinagar, India

Kowsar Majid – Department of Chemistry, National Institute of Technology (NIT), Jammu & Kashmir 190006 Srinagar, India; iDREAM (Interdisciplinary Division for Renewable Energy & Advanced Materials, Laboratory for Bioinspired Research on Advanced Interface and Nanomaterials (BRAINS), NIT, Jammu & Kashmir 190006 Srinagar, India; orcid.org/0000-0001-5760-1809

Mohammad Farooq Wani – Department of Mechanical Engineering, NIT Srinagar, NIT, Jammu & Kashmir 190006 Srinagar, India

Uttam Manna – Department of Chemistry, Indian Institute of Technology (IIT), Guwahati 781039 Assam, India

Gajanan Ghodake – Department of Biological Science and Environmental Science, College of Life Science and Biotechnology, Dongguk University, Goyang-si 10326 Gyeonggi-do, Republic of Korea; orcid.org/0000-0001-6527-3745

Complete contact information is available at:

<https://pubs.acs.org/doi/10.1021/acsomega.3c08417>

Notes

The authors declare no competing financial interest.

■ ACKNOWLEDGMENTS

This work is supported by SERB (Science & Technology Research Board)—a statutory body under the Department of Science & Technology, Government of India, under the research grant of the Ramanujan Fellow Award (file no. SB/S2/RJN-013/2018).

■ REFERENCES

- (1) Singh, H.; Bhardwaj, N.; Arya, S. K.; Khatri, M. Environmental Impacts of Oil Spills and Their Remediation by Magnetic Nanomaterials. *Environ. Nanotechnol., Monit. Manage.* **2020**, *14*, 100305.
- (2) Vüllers, F.; Gomard, G.; Preinfalk, J. B.; Klampaftis, E.; Worgull, M.; Richards, B.; Hölscher, H.; Kavalenka, M. N. Bioinspired Superhydrophobic Highly Transmissive Films for Optical Applications. *Small* **2016**, *12* (44), 6144–6152.
- (3) Pawlak, Z.; Skowron, A. Rudiments of Rough Sets. *Inf. Sci.* **2007**, *177* (1), 3–27.
- (4) Osváth, G.; Daubner, T.; Dyke, G.; Fuisz, T. I.; Nord, A.; Péntzes, J.; Vargancsik, D.; Vágási, C. I.; Vincze, O.; Pap, P. L. How Feathered

Are Birds? Environment Predicts Both the Mass and Density of Body Feathers. *Funct. Ecol.* **2018**, *32*, 701–712.

(5) Amir-Heidari, P.; Arneborg, L.; Lindgren, J. F.; Lindhe, A.; Rosén, L.; Raie, M.; Axell, L.; Hassellöv, I. M. A State-of-the-Art Model for Spatial and Stochastic Oil Spill Risk Assessment: A Case Study of Oil Spill from a Shipwreck. *Environ. Int.* **2019**, *126*, 309–320.

(6) Moyle, P. B.; Leidy, R. A. Loss of Biodiversity in Aquatic Ecosystems: Evidence from Fish Faunas. *Conserv. Biol.* **1992**, 127–169.

(7) Polazzo, F.; Dos Anjos, T. B. O.; Arenas-Sánchez, A.; Romo, S.; Vighi, M.; Rico, A. Effect of Multiple Agricultural Stressors on Freshwater Ecosystems: The Role of Community Structure, Trophic Status, and Biodiversity-Functioning Relationships on Ecosystem Responses. *Sci. Total Environ.* **2022**, *807*, 151052.

(8) Barthlott, W.; Moosmann, M.; Noll, I.; Akdere, M.; Wagner, J.; Røling, N.; Koepchen-Thomä, L.; Azzad, M. A. K.; Klopp, K.; Gries, T.; et al. Adsorption and Superficial Transport of Oil on Biological and Bionic Superhydrophobic Surfaces: A Novel Technique for Oil-Water Separation. *Philos. Trans. R. Soc., A* **2020**, *378* (2167), 20190447.

(9) Zhang, N.; Qi, Y.; Zhang, Y.; Luo, J.; Cui, P.; Jiang, W. A Review on Oil/Water Mixture Separation Material. *Ind. Eng. Chem. Res.* **2020**, *59* (33), 14546–14568.

(10) Song, J.; Huang, S.; Lu, Y.; Bu, X.; Mates, J. E.; Ghosh, A.; Ganguly, R.; Carmalt, C. J.; Parkin, I. P.; Xu, W.; Megaridis, C. M. Self-Driven One-Step Oil Removal from Oil Spill on Water via Selective-Wettability Steel Mesh. *ACS Appl. Mater. Interfaces* **2014**, *6* (22), 19858–19865.

(11) Ribeiro, T. H.; Smith, R. W.; Rubio, J. Sorption of Oils by the Nonliving Biomass of a *Salvinia* Sp. *Environ. Sci. Technol.* **2000**, *34* (24), 5201–5205.

(12) Freudenburg, W. R.; Gramling, R. *Blowout in the Gulf: The BP Oil Spill Disaster and the Future of Energy in America*; MIT Press, 2011.

(13) Wolok, E.; Barafi, J.; Joshi, N.; Girimonte, R.; Chakraborty, S. Study of Bio-Materials for Removal of the Oil Spill. *Arabian J. Geosci.* **2020**, *13*, 1244.

(14) Fingas, M. Physical Spill Countermeasures. In *Oil spill science and technology*; Elsevier, 2011, pp 303–337.

(15) Yong, J.; Huo, J.; Chen, F.; Yang, Q.; Hou, X. Oil/Water Separation Based on Natural Materials with Super-Wettability: Recent Advances. *Phys. Chem. Chem. Phys.* **2018**, *20* (39), 25140–25163.

(16) Zeiger, C.; da Silva, I. C. R.; Mail, M.; Kavalenka, M. N.; Barthlott, W.; Hölscher, H. Microstructures of Superhydrophobic Plant Leaves-Inspiration for Efficient Oil Spill Cleanup Materials. *Bioinspiration Biomimetics* **2016**, *11* (5), 56003.

(17) Liu, J.; Chen, Y.; Zhang, B.; Zhang, Q.; Zhao, D.; Song, J. Superhydrophobic Straw Felt for Oil Absorption. *Results Eng.* **2022**, *13*, 100370.

(18) Mohd, G.; Majid, K.; Lone, S. Multiscale Janus Surface Structure of *Trifolium* Leaf with Atmospheric Water Harvesting and Dual Wettability Features. *ACS Appl. Mater. Interfaces* **2022**, *14* (3), 4690–4698.

(19) Luo, Z. Y.; Chen, K. X.; Wang, J. H.; Mo, D. C.; Lyu, S. S. Hierarchical Nanoparticle-Induced Superhydrophilic and under-Water Superoleophobic Cu Foam with Ultrahigh Water Permeability for Effective Oil/Water Separation. *J. Mater. Chem. A* **2016**, *4* (27), 10566–10574.

(20) Kavalenka, M. N.; Vüllers, F.; Lischker, S.; Zeiger, C.; Hopf, A.; Röhrig, M.; Rapp, B. E.; Worgull, M.; Hölscher, H. Bioinspired Air-Retaining Nanofur for Drag Reduction. *ACS Appl. Mater. Interfaces* **2015**, *7* (20), 10651–10655.

(21) Philippe, A.; Schaumann, G. E. Interactions of Dissolved Organic Matter with Natural and Engineered Inorganic Colloids: A Review. *Environ. Sci. Technol.* **2014**, *48* (16), 8946–8962.

(22) Kharisov, B. I.; Rasika Dias, H. V.; Kharissova, O. V.; Méndez, Y. P. Nanomaterial-Based Methods for Cleaning Contaminated Water in Oil Spill Sites. *Nanotechnol. Energy Sustainability* **2017**, 1139–1160.

(23) Balachandran, A.; Bhat, I. M.; Tabasum, R.; Mohd, G.; Wani, M. F.; Majid, K.; Wahid, M.; Lone, S. Transfer-Printed Environ-

mental-Friendly Anisotropic Filter with Laser-Controlled Micropores for Efficient Oil/Water Separation. *ACS Appl. Polym. Mater.* **2023**, *5* (3), 2272–2281.

(24) Gunning, B. E. S. Microtubules and Cytomorphogenesis in a Developing Organ: The Root Primordium of *Azolla Pinnata*. In *Cytomorphogenesis in plants*; Springer, 1981, pp 301–325.

(25) de Vries, J.; Fischer, A. M.; Roettger, M.; Rommel, S.; Schluemann, H.; Bräutigam, A.; Carlsbecker, A.; Gould, S. B. Cytokinin-Induced Promotion of Root Meristem Size in the Fern *Azolla* Supports a Shoot-like Origin of Euphyllophyte Roots. *New Phytol.* **2016**, *209* (2), 705–720.

(26) Yamasaki, H.; Ogura, M. P.; Kingjoe, K. A.; Cohen, M. F. D-Cysteine-Induced Rapid Root Abscission in the Water Fern *Azolla Pinnata*: Implications for the Linkage between d-Amino Acid and Reactive Sulfur Species (RSS) in Plant Environmental Responses. *Antioxidants* **2019**, *8* (9), 411.

(27) Aziz, A. New Method of Large-Scale Production of *Azolla Pinnata* Var. *Pinnata* R. Brown: A Multipurpose Crop. *Int. J. Appl. Agric. Res.* **2012**, *7*, 1–9.

(28) Munz, P. A. *A Flora of Southern California*; Univ of California Press, 2022.

(29) Barthlott, W.; Schimmel, T.; Wiersch, S.; Koch, K.; Brede, M.; Barczewski, M.; Walheim, S.; Weis, A.; Kaltenmaier, A.; Leder, A.; Bohn, H. F. The *Salvinia* Paradox: Superhydrophobic Surfaces with Hydrophilic Pins for Air Retention Under Water. *Adv. Mater.* **2010**, *22* (21), 2325–2328.

(30) Issa, A. A.; Abd-Alla, M. H.; Ohyama, T. Nitrogen Fixing Cyanobacteria: Future Prospect. *Adv. Biol. Ecol. Nitrogen Fixation* **2014**, *2*, 23–48.

(31) Feng, L.; Zhang, Y.; Xi, J.; Zhu, Y.; Wang, N.; Xia, F.; Jiang, L. Petal Effect: A Superhydrophobic State with High Adhesive Force. *Langmuir* **2008**, *24* (8), 4114–4119.

(32) Dai, X.; Stogin, B. B.; Yang, S.; Wong, T.-S. Slippery Wenzel State. *ACS Nano* **2015**, *9* (9), 9260–9267.

(33) Whyman, G.; Bormashenko, E. How to Make the Cassie Wetting State Stable? *Langmuir* **2011**, *27* (13), 8171–8176.

(34) Zhang, Y.-L.; Xia, H.; Kim, E.; Sun, H.-B. Recent Developments in Superhydrophobic Surfaces with Unique Structural and Functional Properties. *Soft Matter* **2012**, *8* (44), 11217–11231.

(35) Mohd, G.; Majid, K.; Lone, S. Synergetic Role of Nano-/Microscale Structures of the *Trifolium* Leaf Surface for Self-Cleaning Properties. *Langmuir* **2023**, *39*, 6178–6187.

(36) Yang, S.; Ju, J.; Qiu, Y.; He, Y.; Wang, X.; Dou, S.; Liu, K.; Jiang, L. Peanut Leaf Inspired Multifunctional Surfaces. *Small* **2014**, *10* (2), 294–299.

(37) Pan, W.; Ma, J.; Yan, D.; Xu, W.; Chen, Y.; Huang, L.; Song, J. A Facile and High-Efficient Method to Fabricate Slippery Liquid-Infused Porous Surface with Enhanced Functionality. *Surf. Coat. Technol.* **2023**, *472*, 129897.

(38) Pan, W.; Wang, Q.; Ma, J.; Xu, W.; Sun, J.; Liu, X.; Song, J. Solid-Like Slippery Coating with Highly Comprehensive Performance. *Adv. Funct. Mater.* **2023**, *33*, 2302311.